

Antiviral activity and metal ion-binding properties of some 2-hydroxy-3-methoxyphenyl acylhydrazones

M. Carcelli  · E. Fiscaro · C. Compari · L. Contardi ·
D. Rogolino · C. Solinas · A. Stevaert · L. Naesens

Received: 21 November 2017 / Accepted: 24 November 2017
© Springer Science+Business Media, LLC, part of Springer Nature 2017

Abstract Here we report on the results obtained from an antiviral screening, including herpes simplex virus, vaccinia virus, vesicular stomatitis virus, Coxsackie B4 virus or respiratory syncytial virus, parainfluenza-3 virus, reovirus-1 and Punta Toro virus, of three 2-hydroxy-3-methoxyphenyl acylhydrazone compounds in three cell lines (i.e. human embryonic lung fibroblast cells, human cervix carcinoma cells, and African Green monkey kidney cells). Interesting antiviral EC₅₀ values are obtained against

herpes simplex virus-1 and vaccinia virus. The biological activity of acylhydrazones is often attributed to their metal coordinating abilities, so potentiometric and microcalorimetric studies are here discussed to unravel the behavior of the three 2-hydroxy-3-methoxyphenyl compounds in solution. It is worth of note that the acylhydrazone with the higher affinity for Cu(II) ions shows the best antiviral activity against herpes simplex and vaccinia virus (EC₅₀ ~ 1.5 μM, minimal cytotoxic concentration = 60 μM, selectivity index = 40).

Electronic supplementary material The online version of this article (<https://doi.org/10.1007/s10534-017-0070-6>) contains supplementary material, which is available to authorized users.

Keywords Copper complex · Copper homeostasis · Antiviral · Acylhydrazone · Isothermal titration calorimetry

M. Carcelli (✉) · D. Rogolino
Department of Chemistry, Life Sciences and Environmental Sustainability and CIRCMSB (Consorzio Interuniversitario di Ricerca in Chimica dei Metalli nei Sistemi Biologici) Parma Unit, University of Parma, Parco Area delle Scienze 17/A, 43124 Parma, Italy
e-mail: mauro.carcelli@unipr.it

E. Fiscaro · C. Compari · L. Contardi
Food and Drug Department, University of Parma, Parco Area delle Scienze 27/A, 43124 Parma, Italy

C. Solinas
Chemistry and Pharmacy Department, University of Sassari, Via Vienna 2, 07100 Sassari, Italy

A. Stevaert · L. Naesens
Rega Institute for Medical Research, KU Leuven – University of Leuven, 3000 Louvain, Belgium

Introduction

Acylhydrazones are a class of compounds receiving continuous attention in coordination and medicinal chemistry. Even if this is partially due to the often relatively simple synthetic strategies that are used to obtain these compounds, their coordination abilities still hold some interesting surprises (Jiang et al. 2015; Vantomme and Lehn 2013). Recently, metal binding agents were re-discovered as an important tool in bioinorganic chemistry or as drugs to target transition metal ion homeostasis (Chana et al. 2017; Helsel and Franz 2015; Weekley and He 2017). In this context, the *N*-acylhydrazone moiety represents a “privileged

structure”, because of its ability to provide, around a common platform, ligands with different electronic and steric characters. Recently, salicyl-hydrazone analogues have been synthesized and evaluated for their in vitro cytotoxic activities in some human cancer cell lines (Sayed et al. 2017), as well as for antiviral activity (Kim et al. 2016). In the last years, also in our laboratory, studies have been undertaken to assess the antiviral activity of hydroxy-phenyl acylhydrazones (Carcelli et al. 2016; Rogolino et al. 2015); particular attention was devoted to correlate these biological activities with their coordinating abilities. As a follow-up on this work, we here discuss the coordinating behavior of three 2-hydroxy-3-methoxyphenyl acylhydrazones **HL**¹, **HL**², and **H₂L**³ (Scheme 1, R = C₆H₅, C₇H₁₅ and C₆H₄OH) towards some metal ions (Cu(II), Mn(II), Mg(II)), that are essential in living systems. The R group is chosen to diversify the lipophilicity and the coordinating ability of the three compounds. Moreover, here we present the results of the evaluation of **HL**¹, **HL**², and **H₂L**³ in cell cultures infected with diverse DNA or RNA viruses (i.e. herpes simplex virus, vaccinia virus, vesicular stomatitis virus, Coxsackie B4 virus or respiratory syncytial virus, parainfluenza-3 virus, reovirus-1 and Punta Toro virus), revealing interesting activities against herpes simplex virus and vaccinia virus.

Experimental

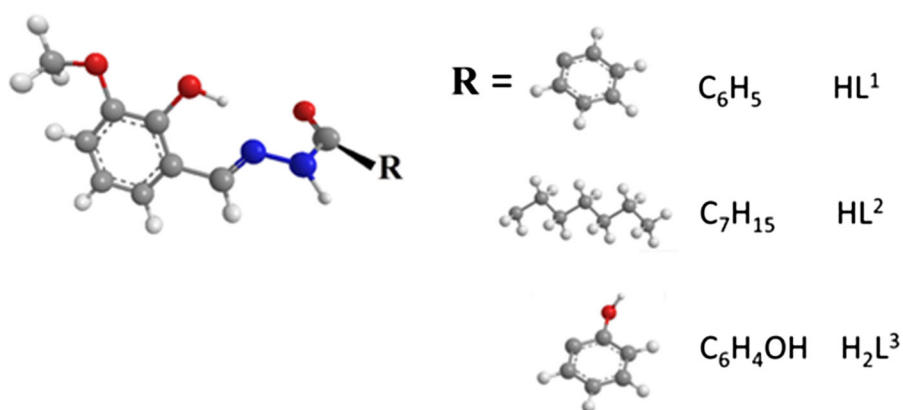
Materials and methods

All reagents of commercial quality were used without further purification. The purity of the synthesized compounds was determined by elemental analysis and verified to be $\geq 95\%$. NMR spectra were recorded at 25 °C on a Bruker Avance 400 FT spectrophotometer. The attenuate total reflectance IR spectra were recorded by means of a Nicolet-Nexus (Thermo Fisher) spectrophotometer by using a diamond crystal plate in the range of 4000–400 cm⁻¹. Elemental analyses were performed by using a FlashEA 1112 series CHNS/O analyzer (Thermo Fisher) with gas-chromatographic separation. Electro spray mass spectral analyses (ESI-MS) were performed with an electrospray ionization time-of-flight Micromass 4LCZ spectrometer. MS spectra were acquired in positive EI mode by means of a direct exposure probe mounting on the tip of a Re-filament with a DSQII Thermo Fisher apparatus, equipped with a single quadrupole analyzer.

Chemistry

N'-(2-hydroxy-3-methoxybenzylidene)benzoylhydrazide (**HL**¹) (Pouralimardan et al. 2007), *N'*-(2-hydroxy-3-methoxybenzylidene)heptylhydrazide (**HL**²) (Carcelli et al. 2016), and *N'*-(2-hydroxy-3-methoxybenzylidene)-2-hydroxybenzoylhydrazide (**H₂L**³) (Rogolino et al. 2015) were synthesized following literature methods. Briefly, to a solution of 2-hydroxy-3-methoxybenzaldehyde in absolute ethanol, an equimolar amount of the proper

Scheme 1 Molecular structure of the 2-hydroxy-3-methoxyphenyl acylhydrazones **HL**¹, **HL**², and **H₂L**³



hydrazide in the same solvent was added. The mixture was refluxed for 6 h, cooled at room temperature and concentrated in vacuum. The precipitate was filtered off, washed with cold ethanol and dried in vacuum. The scheme of the synthesis and the characterizations of **HL**¹, **HL**² and **H₂L**³ are reported in the Supplementary Data.

Potentiometric titrations

The procedure for potentiometric titration is described in full details elsewhere (Fiscaro and Braibanti 1988; Gran 1952). Briefly, equilibrium constants for protonation and complexation were determined by means of potentiometric titrations in methanol:water = 9:1 v/v solutions, ionic strength 0.1 mol dm⁻³ KCl. Titrations were carried out under nitrogen in the pH range 3–11 by using a fully automated apparatus; temperature (25 ± 0.1 °C) was controlled to ± 0.1 °C by using a thermostatic circulating water bath (ISCOGTR 2000 IIX). The electrodic chain (Crison 5250 glass electrode and 0.1 mol dm⁻³ KCl in methanol:water = 9:1 v/v calomel electrode, Radiometer 401) was calibrated in terms of [H⁺] by means of a strong acid–strong base titration by Gran's method (Gran 1952) (E° = 371.5 ± 0.4 mV, pK_w = 14.40 ± 0.05). Appropriate aliquots of ligand solution, prepared by weight, with and without metal ions, were titrated with a KOH solution (methanol:water = 9:1 v/v, I = 0.1 mol dm⁻³ KCl), whose titre was determined by using potassium phthalate as primary standard. The concentrations of the Mg(II) and Mn(II) stock solutions (from MgCl₂·6H₂O and MnCl₂·4H₂O) were determined by using EDTA, the sodium salt of Eriochrome black T and NH₃/NH₄Cl as a buffer. The concentration of the Cu(II) stock solution (from CuCl₂·2H₂O) was determined by using EDTA in the

presence of concentrated ammonia by using Fast Sulfon Black as indicator. Metals solutions were acidified by adding HCl to avoid hydrolysis. The concentration of the excess H⁺ was obtained by titrating with standard KOH solution. The protonation constants of **HL**¹ and **HL**² were obtained by titrating 20 ml of samples of each ligand (3 × 10⁻³ 0.1 mol dm⁻³). For obtaining the complex formation constants, titrations were performed in different ligand/metal ratios (from 1 up to 4). At least two measurements (about 60 experimental points each) were performed for each system. The software HYPERQUAD (Gans et al. 1996) was used for extracting the speciation and the logarithm of the stability constants (log β_{pqr}) from experimental titration data. β_{pqr} = [M_pL_qH_r]/[M]^p[L]^q[H]^r indicates the cumulative formation constant for the equilibrium pM + qL + rH ⇌ M_pL_qH_r, where M is the metal, L the completely deprotonated ligand and H the proton. Charges are omitted for simplicity.

Isothermal titration calorimetry (ITC)

ITC measurements were carried out on a CSC model 5300 N-ITC III isothermal titration calorimeter (Calorimetry Sciences Corporations, USA) at 25 °C. KOH solution (0.065–0.145 mol dm⁻³) in methanol:water = 9:1 at 0.1 mol dm⁻³ KCl ionic strength was injected in steps of 5 μL into a 960 μL reaction cell by a 250 μL syringe with an interval of 400–500 s between two successive injections, with stirring speed of 150 revolutions per minute (rpm), following the procedure previously described (Fiscaro et al. 2014). For obtaining the protonation heat of the ligand, the cell was filled up with a solution of the ligand in methanol:water = 9:1, 0.1 mol dm⁻³ KCl ionic strength. Dilution heats were subtracted by carrying out blank experiments, in which the KOH

Scheme 2 (left) The coordinating motif of **HL**¹, **HL**² and **H₂L**³; (right) four deprotonated hydroxyl hydrogens of four ligands bridge the copper(II) ions. The four oxygens and the four copper(II) ions form the molecular core of a Cu₄(ligand)₄ complex

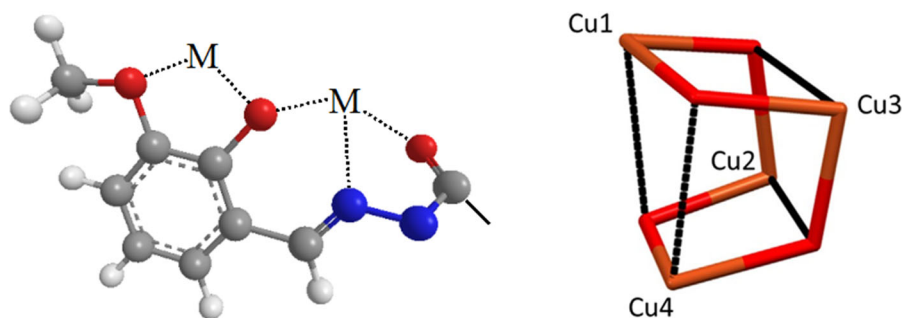


Table 1 Thermodynamic parameters for the protonation of the ligands under study at 298 K

	$\log \beta_{011}$	ΔG^\ominus (kJ mol ⁻¹)	ΔH^\ominus (kJ mol ⁻¹)	ΔS^\ominus (kJ mol ⁻¹)
HL¹	10.63 (1)	- 60.72 (2)	- 15.7 (7)	151 (4)
HL²	11.18 (1)	- 63.9 (2)	- 11.1 (2)	177 (3)
HL³ $\log \beta_{011}$	12.11 (1)	- 69.1 (2)	- 16.6 (7)	176 (10)
$\log \beta_{012}$	20.54 (1)	- 117.2 (2)	- 24.5 (7)	311 (10)

In brackets the standard deviation on the last figure

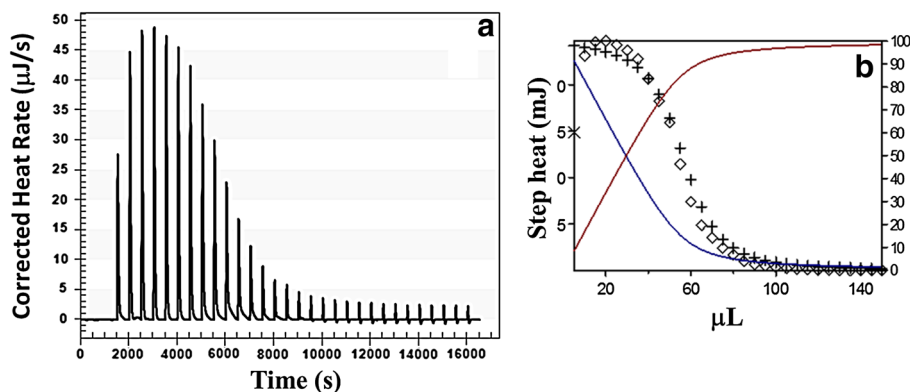


Fig. 1 **a** Raw data from the ITC titration for the protonation of **HL¹**. Upward peaks indicate an exothermic reaction. Each peak corresponds to a single 5 μ l injection. **b** Comparison between experimental (\diamond) and computed (+) stepwise heats (output from Hyp Δ H software). Experimental conditions: 5.7

μ moles of **HL¹** in the cell, titrant KOH 0.1 mol dm⁻³, both in MeOH:H₂O = 9:1 and KCl 0.1 mol dm⁻³. The molar fraction of **HL¹** (blue curve) and of **L¹** (red curve) are also shown versus titrant volume in μ l. (Color figure online)

solution was injected into the same solvent, without ligand. The molar enthalpy change for the reaction $H^+ + OH^- \rightleftharpoons H_2O$ was obtained by titrating a solution of HCl (in the cell) by KOH, in the burette, both prepared in methanol:water = 9:1 at ionic strength 0.1 mol dm⁻³ KCl. It results -20.6 ± 0.4 kJ mol⁻¹ (Fiscaro et al. 2014). The experimental peaks were integrated and corrected for the dilution heats by the NanoAnalyze (TA Instrument) software. The data so obtained were elaborated by the Hyp Δ H software (Gans et al. 2008), assuming the protonation constants from potentiometric measurements.

Cells and viruses

The antiviral cytopathic effect (CPE) reduction assays were performed in three different cell lines infected with diverse DNA or RNA viruses (see [Antiviral activity](#) for specific names of cells and viruses) (Rogolino et al. 2015). These experiments

were performed in 96-well plates containing semi-confluent cell cultures to which 100 CCID₅₀ (50% cell culture infective dose) of virus was added together with serial dilutions of the compounds. When maximal CPE was reached, i.e. at 3–6 days post infection, microscopy was performed to score the virus-induced CPE. Compound cytotoxicity was also determined by microscopy, using a mock-infected plate.

Results and discussion

HL¹, **HL²** and **H₂L³** share a common synthon, the 3-methoxysalicyl aldehyde; when it is reacted with an hydrazide, a coordinating environment is formed with two sites, an *OO'* bidentate and an *ONO'* tridentate one. The solid state X-ray characterization of the complexes of this type of ligands with Cu(II) and Mn(II) is sufficiently extended. In particular, two types of species have been isolated, both of them with a 1/1

Table 2 Logs of the protonation and the complexes formation constants ($\beta_{pqr} = [M_p L_q H_r]/[M]^p [L]^q [H]^r$) of the ligands **HL**¹ and **HL**² and **H(HL**³) (for comparison purposes **H₂L³** is here

considered monoprotic, so that $L = HL^3$) with Mg(II), Mn(II) and Cu(II), in the mixed solvent MeOH:H₂O = 9:1

p	q	r	HL ¹	HL ²	H(HL ³)
0	1	1	10.63 (1)	11.18 (1)	8.43 (1)
Mg(II)					
1	1	0	5.04 (4)	5.29 (6)	2.8 (2)
1	2	0	9.45 (3)	9.47 (4)	
Mn(II)					
1	1	0	7.1 (1)	7.7 (1)	5.34 (7)
1	2	0	12.0 (4)	13.3 (3)	
Cu(II)					
1	1	0	12.0 (3)	11.84 (6)	
1	1	-1	7.6 (3)	6.41 (6)	1.84 (1)
1	2	-1	10.9 (3)	10.12 (7)	
1	2	-2	-0.8 (3)	-2.03 (7)	

Standard deviations on the last figure are shown in brackets

metal/ligand *ratio*: depending on the reaction conditions, it is possible to obtain a dimetallic, dimer complex (Scheme 2) (Ray et al. 2009; Vrdoljak et al. 2016) or, in the case of Cu(II), a tetrameric complex (Ray et al. 2009; Rogolino et al. 2015).

On the contrary, the solution chemistry of **HL**¹, **HL**² and **H₂L³** is relatively undeveloped. We are particularly interested in their speciation with metal ions that are relevant for biological activity, as Cu(II), Mn(II) and Mg(II). For this reason, potentiometric titrations were carried out in mixed solvent methanol/water = 9/1 (ionic strength = 0.1 mol dm⁻³ KCl), where these ligands are soluble in the millimolar range, to be consistent with our previous studies about ligand of pharmaceutical interest but poorly soluble in water (Bacchi et al. 2011; Rogolino et al. 2014, 2015). First, the protonation constants of the ligands were determined. The pK_as are 10.63(1) for **HL**¹, 11.18(1) for **HL**², and 8.43(1) and 12.11(1) (Rogolino et al. 2015) for **H₂L³**. It seems reasonable to consider that the 2-hydroxy group is the first one to dissociate (Ali Kamyabi et al. 2008). Effectively, **HL**¹ and **HL**² are diprotic (OH and NH), and in **H₂L³** another OH group is present, but the methanol/water (9/1) solvent seems to lower acidity so that the higher pK_a is not detected by potentiometric titration.

The thermodynamics of the protonation of the three ligands were determined by ITC experiments,

allowing evaluation of the enthalpic and entropic components (Eqs. 1 and 2):

$$\Delta G^0 = -RT \ln \beta_{pqr} \quad (1)$$

$$\Delta G^0 = \Delta H^0 - T\Delta S^0 \quad (2)$$

The experimental heats from isothermal calorimetry titration, subtracted of the dilution heats, were processed by HypΔH software (Gans et al. 2008), assuming the protonation constants from the potentiometric measurements. Results are reported in Table 1. The protonation of all the ligands is favored from both the entropic and the enthalpic factors. In Fig. 1, an example of a microcalorimetric titration output and the comparison between experimental and computed stepwise heats for **HL**¹ from the HypΔH output are shown. Data for **HL**² and **H₂L³** are presented in the Supplementary Data.

As far as the formation of the complexes between **HL**¹ and **HL**² and Mg²⁺ and Mn²⁺ metal ions is concerned, unfortunately we had to deal with poor solubility of the species formed in solution, especially with Mn²⁺ ions. The solution started to become turbid in the range 8 < pH < 11 for **HL**¹ and 7.5 < pH < 11.5 for **HL**², with metal:ligand *ratio* 1:2. At higher pH the precipitate dissolved again. When Mg²⁺ is considered, the solutions were cloudy at pH > 8.5. Obviously, only the experimental points

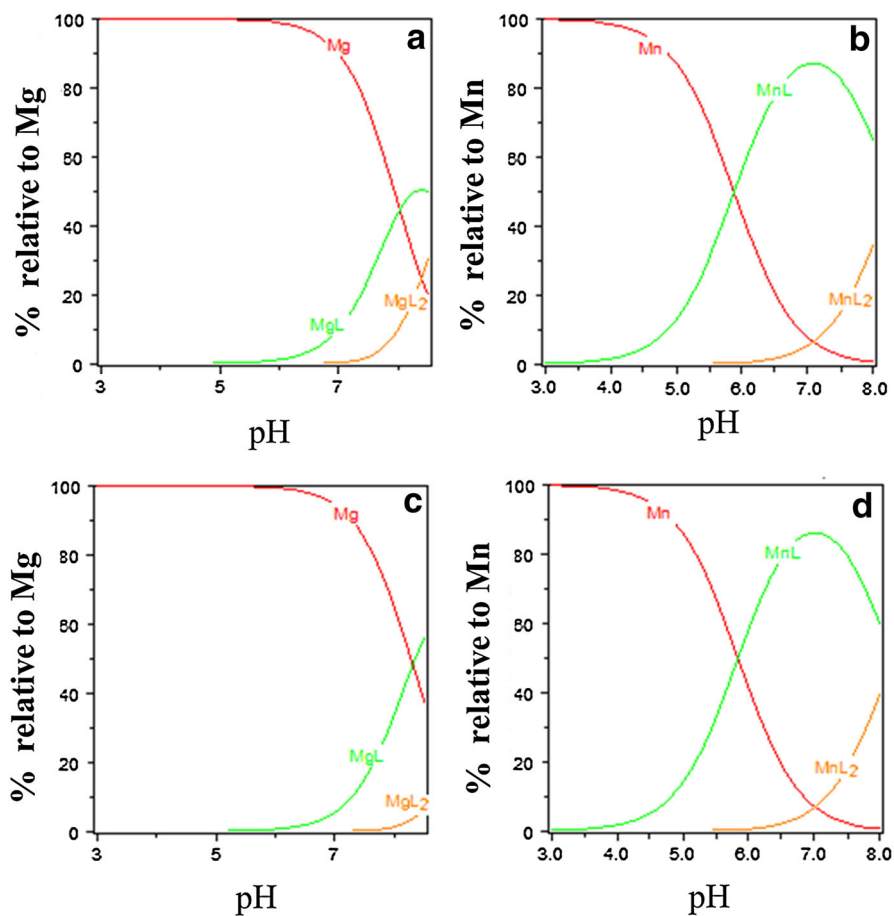


Fig. 2 Distribution diagrams for the systems ligand:M(II) = 4:1 (M(II) concentration = 1.25×10^{-3} mol dm⁻³). (a) $\text{HL}^1\text{-Mg(II)}$; (b) $\text{HL}^1\text{-Mn(II)}$; (c) $\text{HL}^2\text{-Mg(II)}$; (d) $\text{HL}^2\text{-Mn(II)}$. Charges were omitted for simplicity

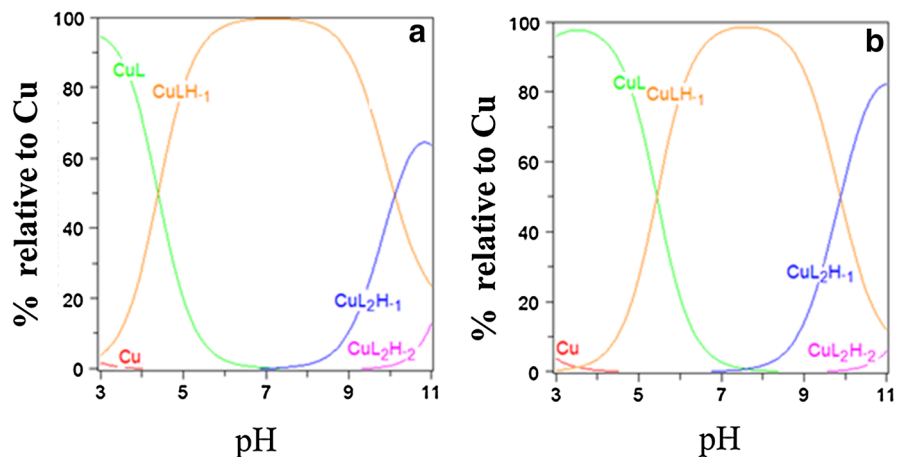


Fig. 3 Distribution diagrams for the systems ligand:Cu(II) = 4:1 (Cu(II) concentration = 1.25×10^{-3} mol dm⁻³). (a) $\text{HL}^1\text{-Cu(II)}$; (b) $\text{HL}^2\text{-Cu(II)}$. Charges were omitted for simplicity

Table 3 Antiviral activity of **HL**¹, **HL**², and **H₂L**³ in cell culture assays

Compound	Antiviral EC ₅₀ ^a (μM) in HEL cells infected with			Minimal cytotoxic concentration ^b (μM) in		
	Herpes simplex virus-1	Vaccinia virus	Adenovirus type 2	HEL	HeLa	Vero
HL ¹	6.4	6.8	> 100	≥ 100	20	≥ 20
HL ²	8.9	8.9	> 100	≥ 100	20	> 100
H₂L ³	1.6	1.3	> 100	60	4	20
Cidofovir ^c	0.95	16	7.9	> 250	nd	nd

Cell lines used: HEL, human embryonic lung fibroblast cells; HeLa, human cervix carcinoma cells; Vero, African Green monkey kidney cells

^a EC₅₀: 50% effective concentration, i.e. compound concentration producing 50% inhibition of virus-induced CPE, determined by microscopy. Compounds are not active against: vesicular stomatitis virus, Coxsackie B4 virus or respiratory syncytial virus (assessed in HeLa cells), parainfluenza-3 virus, reovirus-1 and Punta Toro virus (assessed in Vero cells)

^b Compound concentration producing minimal alterations in cell morphology, determined by microscopy

^c Cidofovir used as reference drug

nd not done

in which the solution appeared clear were processed by using HYPERQUAD software (Gans et al. 1996). The models of speciation showing the best statistical parameters and the best fit between experimental and computed potentiometric titration curves are shown in Table 2. The distribution diagrams as a function of pH, evaluated for metal to ligand ratio = 4:1, are reported in Fig. 2. It can be gathered that the insoluble species is ML₂, the neutral one. For Mn(II), we processed also the points at the highest pH in which the solution was clear, and we were able to find out the species MnL₂¹H₋₁ [log β_{1 2 -1} = 0.8(4)] and MnL₂¹H₋₂ [log β_{1 2 -2} = - 11.3(6)] and, similarly for the other ligand, MnL₂²H₋₁ [log β_{1 2 -1} = 2.0(4)] and MnL₂²H₋₂ [log β_{1 2 -2} = - 11.8(4)], with high confidence. These species, not reported in Table 2 because they form at a pH in which it is generally assumed that the glass electrode does not work perfectly, explain the redissolution at high pH. They are probably hydroxylated species derived from the dissociation of water molecule in the inner coordination sphere.

The Cu(II) ion showed higher affinity for the ligands and a different behavior was observed in solution. For example, the systems with Cu(II) and **HL**¹ and **HL**² were clear all through the examined pH range, before becoming pale yellow and then turning to pale green at higher pH. The species giving rise to the best fit between computed and experimental titrations, reported in Table 2, suggest that Cu(II)

enhances very much the acidity of the hydrazonic nitrogen, so that a bidentate NO chelate forms in the inner coordination sphere. The distribution diagrams as a function of the pH for Cu(II):ligand = 4:1, are shown in Fig. 3. Comparison of the distribution diagrams in Figs. 2 and 3 clearly proves that the complexation of Cu(II) starts already at low pH, unlike that of Mg(II) and Mn(II), due to the pronounced difference in affinity. The presence of another phenolic OH group in **H₂L**³ enhance the affinity for Cu(II) ions (Table 2) and in addition allows the formation of polynuclear species, as elsewhere discussed and also characterized by single crystal X ray diffraction (Rogolino et al. 2015).

Antiviral activity

The three compounds **HL**¹, **HL**² and **H₂L**³ underwent broad antiviral evaluation against a variety of DNA and RNA viruses, in three cell lines, i.e. human embryonic lung (HEL) fibroblast cells, human cervix carcinoma cells (HeLa), and African Green monkey kidney cells (Vero). Interestingly, in the HEL assays, the three compounds displayed activity against the enveloped DNA viruses herpes simplex virus type 1 and vaccinia virus, yet were inactive against adenovirus, a naked DNA virus. **H₂L**³ was the most active one, with an antiviral EC₅₀ value of ~ 1.5 μM and a minimal cytotoxic concentration of 60 μM, yielding a favourable selectivity index (ratio of cytotoxic to

antiviral concentration) of 40. About 5-fold lower activity and selectivity was seen with the other two molecules, **HL**¹ and **HL**². Neither of the three compounds was active against any of the other viruses, i.e. vesicular stomatitis virus, Coxsackie B4 virus or respiratory syncytial virus, assessed in HeLa cells, and parainfluenza-3 virus, reovirus-1 and Punta Toro virus, assessed in Vero cells (data not shown). Finally, we noticed that the cytotoxicity of the compounds was more pronounced in Vero and, in particular, HeLa cells, when compared to HEL cells (Table 3).

Conclusions

The polydentate acylhydrazonic molecules **HL**¹, **HL**² and **H₂L**³ are able to interact with some essential metal ions as Mg(II), Mn(II) and Cu(II). Depending on the R group (Scheme 1) in their structure, the coordinating behavior is different. Despite some solubility problems, it is possible to say that these ligands in general and **H₂L**³ in particular show a preference for Cu(II). It is perhaps premature to correlate the higher affinity of **H₂L**³ for Cu(II) with its good antiviral activity against herpes simplex and vaccinia virus ($EC_{50} \sim 1.5 \mu\text{M}$, minimal cytotoxic concentration = $60 \mu\text{M}$, selectivity index = 40), but the idea of antivirals that can act by perturbation of copper homeostasis (Bleichert et al. 2014; Warnes and Keevil 2013) is fascinating and deserve further experimental efforts.

Acknowledgements “Centro Interdipartimentale Misure Giuseppe Casnati” of the University of Parma is thanked for facilities.

Author’s contributions The manuscript was written through contributions of all authors. All authors have given approval to the final version of the manuscript.

References

- Ali Kamyabi M, Shahabi S, Hosseini-Monfared H (2008) Spectrophotometric and potentiometric study of (E)-N'-(2-hydroxy-3-methoxybenzylidene)benzohydrazide with a ferric ion in the methanol–water mixture. *J Chem Eng Data* 53:2341–2345
- Bacchi A, Carcelli M, Compari C, Fiscaro E, Pala N, Rispoli G, Rogolino D, Sanchez TM, Sechi M, Neamati N (2011) HIV-1 IN strand transfer chelating inhibitors: a focus on metal binding. *Mol Pharm* 8:507–519
- Bleichert P, Espirito Santo Ch, Hanczaruk M, Meyer H, Grass G (2014) Inactivation of bacterial and viral biothreat agents on metallic copper surfaces. *Biometals* 27:1179–1189
- Carcelli M, Rogolino D, Gatti A, De Luca L, Sechi M, Kumar G, White SW, Stevaert A, Naesens L (2016) N-acylhydrazones inhibitors of influenza virus PA endonuclease with versatile metal binding modes. *Sci Rep* 6:31500
- Chana AN, Shiverb AL, Weverc WJ, Zeenat S, Razvid A, Traxlere MF, Lia B (2017) Role for dithiolopyrrolones in disrupting bacterial metal homeostasis. *PNAS* 114:2717–2722
- Fiscaro E, Braibanti A (1988) Potentiometric titrations in methanol/water medium: intertitration variability. *Talanta* 10:769–774
- Fiscaro E, Compari C, Bacciottini F, Contardi L, Carcelli M, Rispoli G, Rogolino D (2014) Thermodynamics of complexes formation by ITC in methanol/water = 9/1 (v/v) solution: a case study. *Thermochim Acta* 586:40–44
- Gans P, Sabatini A, Vacca A (1996) Investigation of equilibria in solution. Determination of equilibrium constants with HYPERQUAD suite of programs. *Talanta* 43:1739–1753
- Gans P, Sabatini A, Vacca A (2008) Simultaneous calculation of equilibrium constants and standard formation enthalpies from calorimetric data for systems with multiple equilibria in solution. *J Solut Chem* 37:467–476
- Gran P (1952) Determination of the equivalence point in potentiometric titrations. Part II. *Analyst* 77:661–671
- Helsel ME, Franz KJ (2015) Pharmacological activity of metal binding agents that alter copper bioavailability. *Dalton Trans* 44:8760–8770
- Jiang Q, Sicking W, Ehlers M, Schmuck C (2015) Discovery of potent inhibitors of human β -tryptase from pre-equilibrated dynamic combinatorial libraries. *Chem Sci* 6:1792–1800
- Kim B, Ko H, Jeon E, Ju E, Jeong LS, Kim Y (2016) 2,3,4-Trihydroxybenzyl-hydrazide analogues as novel potent coxsackievirus B3 3C protease inhibitors. *Eur J Med Chem* 120:202–216
- Pouralimardan O, Chamayou A, Janiak Ch, Hosseini-Monfared H (2007) Hydrazone Schiff base-manganese(II) complexes: synthesis, crystal structure and catalytic reactivity. *Inorg Chim Acta* 360:1599–1608
- Ray A, Rizzoli C, Pilet G, Desplanches C, Garrriba E, Rentschler E, Mitra S (2009) Two new supramolecular architectures of singly phenoxo-bridged copper(II) and doubly phenoxo-bridged manganese(II) complexes derived from an unusual ONOO donor hydrazone ligand: syntheses, structural variations, cryomagnetic, DFT, and EPR studies. *Eur J Inorg Chem* 20:2915–2928
- Rogolino D, Carcelli M, Compari C, De Luca L, Ferro S, Fiscaro E, Rispoli G, Neamati N, Debyser Z, Christ F, Chimirri A (2014) Diketoacid chelating ligands as dual inhibitors of HIV-1 integration process. *Eur J Med Chem* 78:425–430
- Rogolino D, Carcelli M, Bacchi B, Compari C, Contardi L, Fiscaro E, Gatti A, Sechi M, Stevaert A, Naesens L (2015) A versatile salicyl hydrazonic ligand and its metal complexes as antiviral agents. *J Inorg Biochem* 150:9–17

- Sayed AM, Choi S, Lee D (2017) Synthesis, anticancer, and docking studies of salicyl-hydrazone analogues: a novel series of small potent tropomyosin receptor kinase A inhibitors. *Bioorg Med Chem* 25:389–396
- Vantomme G, Lehn J (2013) Photo- and thermoresponsive supramolecular assemblies: reversible photorelease of K^+ ions and constitutional dynamics. *Angew Chem Int Ed* 52:3940–3943
- Vrdoljak V, Pavlovic´ G, Maltar-Strmec`ki N, Cindric´ M (2016) Copper(II) hydrazone complexes with different nuclearities and geometries: synthetic methods. *New J Chem* 40:9263–9274
- Warnes SL, Keevil CW (2013) Inactivation of Norovirus on dry copper alloy surfaces. *PLoS ONE* 8:e75017
- Weekley CM, He C (2017) Developing drugs targeting transition metal homeostasis. *Curr Op Chem Biol* 37:26–32